Triaxial Characterization of High-Strength Portland Cement Concrete

MICHAEL I. HAMMONS AND BILLY D. NEELEY

Triaxial characterization tests were conducted on a high-strength portland cement concrete proportioned from readily available materials. The objective was to develop mechanical response data for this high-strength concrete along selected stress and strain paths in multiaxial stress space. The concrete chosen for testing had a water-cement ratio of 0.23 and an unconfined compressive strength at 56 days of 105 MPa. The triaxial test specimens were 50-mm nominal diameter right circular cylinders. All tests were performed in a 276-MPa-capacity cylindrical triaxial cell in conjunction with a 1340 kN-capacity servohydraulic materials testing system. Confining pressure was generated by an external 600-MPa-capacity, air-driven hydraulic pumping system. Active measurements attempted for each test included vertical and horizontal strain, testing machine displacement, axial load, and confining pressure. Triaxial shear tests were conducted at confining pressures of 50, 100, 150, and 200 MPa, and uniaxial strain tests were conducted to a principal stress difference of 350 MPa. These stress-strain data were plotted, and a failure envelope was developed. The test data show that high-strength portland cement concrete is capable of large plastic strains and ductile flow under states of high confinement. The material exhibited strain-softening behavior at the 50-MPa level; thus, it appears that the brittle-ductile transition for the material lies between the 50- and 100-MPa confining stress levels. At confining stresses of 100 MPa and greater, the material behavior is characterized by a strain-hardening ductile behavior to axial strains of 10 percent or greater.

Recent advances in concrete technology have made possible the development and placement of high-strength concrete for civil and military applications. The Concrete Technology Division of the Structures Laboratory at the U.S. Army Engineer Waterways Experiment Station has been developing concretes and binder systems, design procedures, and construction technology to enhance the survivability of hardened facilities (*1–4*). This paper documents the characterization of a high-strength portland cement (HSPC) concrete for use in projectile penetration studies involving various high-strength target materials (*5,6*). With increasing confinement, the strength and ductility of concrete increases dramatically. HSPC concrete should offer better penetration resistance than conventional-strength concretes because of enhanced mechanical properties.

The objective of this research was to develop mechanical response data along selected stress and strain paths in multiaxial stress space. This data will be used by analytical modelers as input into constitutive models for material response calculations.

Concrete Technology Division, Structures Laboratory, U.S. Army Engineer Waterways Experiment Station, 3909 Halls Ferry Road, Vicksburg, Miss. 39190.

A series of triaxial shear and uniaxial strain tests were conducted in a cylindrical triaxial cell to characterize the mechanical response of the material. Triaxial shear tests were conducted on these two mixtures at confining pressures of 50, 100, 150, and 200 MPa, and uniaxial strain tests were conducted to a principal stress difference of 350 MPa. These stress-strain data were plotted, and a failure envelope was developed.

CONCRETE MIXTURE

The project requirements called for an HSPC concrete having as high an unconfined compressive strength as convenient using available materials. The concrete mixture selected for characterization, designated PP/HSPC-1 is described in Table 1. This mixture had a water-cement ratio of 0.23 and an unconfined compressive strength at 56 days age of 105 MPa. Other fresh and hardened properties of the mixture are given in Table 2.

TEST DEVICES AND PROCEDURES

Specimen Preparation

The concrete was batched in the laboratory. Three 0.15- × 0.15- × 0.9-m prisms were cast using extended external mechanical vibration on a vibrating table. The concrete was vibrated until no air was observed coming to the top or until the mixture began to bleed. This technique produced concrete from which cores could be taken that would be expected to be adequately free of large voids. The prisms were cured for 56 days in a moist curing room.

The triaxial test specimens were 50-mm nominal diameter right circular cylinders cored from the prisms. Each core was brushed with a stiff wire brush to expose surface voids. The voids were then filled with gypsum cement to minimize the possibility of membrane puncture during testing.

The sides of the specimens were required to be smooth and free of any abrupt irregularities. The departure from perpendicularity was required to be less than 0.25 degrees. The straightness of the sides was determined by a dial gauge. Measurements were made at each end and at the quarter points on four axes 90 degrees apart. Planeness of the specimen ends was required to be within 0.025 mm. This requirement was checked by making four equally distributed measurements on each of the specimens with a dial gauge. An average diameter and length were computed for each speci-

TABLE 1 Concrete Mixture Proportions, Saturated Surface Dry Conditions: PP/HSPC-1

Item	Proportions, kg/m³
Type I portland cement	1,517
Silica fume	202
Class F fly ash	337
9.5-mm limestone coarse aggregate	2,321
Limestone fine aggregate	1,866
Water	472
High-range water-reducing admixture (powder)	32.9
Air-detraining agent (powder)	3.0

TABLE 2 Fresh and Hardened Properties: PP/HSPC-1

Property	Value
Slump, mm	200
Unit Weight, kg/m³	2,365
Air Content, percent	3.5
Compressive Strength, MPa	
7 days	85
28 days	96
56 days	105
Direct Tensile Strength, MPa	
56 days	5.4
Tensile Elastic Modulus*, MPa	
56 days	44,000
Tensile Strain at Failure, millionths, 56 days	135

*Test method described by Hammons et al.[6].

men, and these values were used as the pretest dimensions of the specimens.

All specimens were air-dried in the laboratory for a sufficient amount of time to equilibrate with the laboratory environment; therefore, all specimens were essentially free of pore water. The specimens were prepared for testing by placing hardened steel-bearing blocks on each end and encasing the specimen in an impermeable membrane. A 60-durometer neoprene tubing was then placed over the specimen and bearing blocks to serve as a flexible membrane. The membrane was secured at each end with hose clamps.

Triaxial Test Device and Procedure

Triaxial properties of concrete are determined generally from two types of test devices: cylindrical triaxial cells and truly triaxial (cubical) cells. This paper is concerned with cylindrical triaxial tests only. In the cylindrical triaxial test device, an axisymmetric stress state exists with two of the three principal stresses being necessarily equal. For this research all tests were performed in a 276-MPa-capacity cylindrical triaxial cell in conjunction with a 1340- kN-capacity servohydraulic materials testing system. This cell accepts a maximum specimen length of approximately 90 mm. Up to four channels of instrumentation can exit the pressure vessel through Fusite fittings in the base.

Confining pressure was generated by an external 600-MPa-capacity, air-driven hydraulic pumping system. The pumping system was connected through high-pressure tubing to a pressure port in the devices. A pharmaceutical-grade mineral oil was used as the confining medium. The loading ram was driven by the servocontrolled hydraulic materials testing system.

After the specimen was placed in the triaxial cell, the assembly was placed under the materials testing system. The confining pressure was increased by means of the pumping system and regulated by hand-operated valves. The universal testing machine provided the axial stress, and the confining pressure was maintained with the hydraulic pump and valve. The test proceeded in a stepwise manner along the prescribed stress or strain path.

After each test was completed, the test device was removed from the testing machine and disassembled. The specimen was recovered, and any anomalies were noted.

Instrumentation

Active measurements attempted for each test included vertical and horizontal strain, testing machine displacement, axial load, and confining pressure. Four foil-strain gauges were applied to each specimen at mid-height. Two vertical gauges were placed diametrically opposite, and two horizontal gauges were placed diametrically opposite on a diameter 90 degrees from the vertical gauges. The two gauges in each orientation were wired in series, and signal conditioners were set to average the data.

The testing machine crosshead displacement was assured by means of a linear motion potentiometer mounted directly on the testing machine. Axial stresses were measured by the load cell on the universal testing machine (corrected for friction on the piston seals) and confining stresses by a pressure transducer in the hydraulic loading system.

All data were recorded on Hewlett Packard Series 200 or 300 computers controlling digital data acquisition hardware. All voltage measurements were preconditioned and amplified using Wheatstone bridge conditioners.

CHARACTERIZATION TEST RESULTS

Project requirements dictated that the mechanical response of the concrete mixtures be characterized along two types of multiaxial paths: triaxial shear and uniaxial strain. Boundary conditions for these tests are described in the following.

Triaxial shear is defined as a stress state described by the following stress tensor, σ:

$$\sigma = \begin{pmatrix} \sigma_{11} & 0 & 0 \\ 0 & \sigma_{33} & 0 \\ 0 & 0 & \sigma_{33} \end{pmatrix}$$

where σ_{11} is the stress in the direction of the axis of the cylinder (herein referred to as "axial stress") and σ_{33} is the confining stress. Because of the boundary conditions of the cylindrical triaxial device, two of the three principal stresses are necessarily equal; therefore, confining stress = $\sigma_{22} = \sigma_{33}$.

The triaxial shear tests were conducted by increasing all three principal stresses isotropically until the desired level of confining stress was obtained. Subsequently, the confining stress was maintained while the axial stress was increased until the test was halted. The criteria for halting a test were as follows:

- Attaining a total axial strain of 10 percent, or
- Reaching ultimate axial stress capacity.

During the course of the triaxial shear tests, considerable barreling of the test specimens occurred at large strains. The axial stress in each test was calculated as the axial load divided by the current cross-sectional area. This definition of axial stress may not be consistent with large deformation theory. Also, as bulging occurs, a component of confining stress becomes directed vertically, causing a stress distribution that becomes quite complex.

A uniaxial strain test is defined by the boundary condition

$$\varepsilon = \begin{pmatrix} \varepsilon_{11} & 0 & 0 \\ 0 & 0 & 0 \\ 0 & 0 & 0 \end{pmatrix}$$

where ε is the engineering strain tensor and ε_{11} is the engineering strain along the axis of the cylinder. These boundary conditions are maintained by manipulating the confining stresses to force $\varepsilon_{22} = \varepsilon_{33} = 0$ as ε_{11} varies.

Triaxial shear tests for the two concretes were conducted at confining stress levels of 50, 100, 150, and 200 MPa, and two uniaxial strain tests were conducted on each mixture. Selected data plots are given in the text of this paper.

Test Results

Table 3 gives a summary of the maximum stress levels obtained during each test. Also reported in the table are maximum values of principal stress difference (PSD), defined as

$$\text{PSD} = \sigma_{11} - \sigma_{33}$$

and mean normal stress (MNS), defined as

$$\text{MNS} = \frac{\sigma_{11} + 2\sigma_{33}}{3}$$

The MNS is a measure of the hydrostatic component of the applied stress, whereas the PSD is a measure of the shear component of the applied stress state. For the cylindrical triaxial test boundary conditions, volumetric strain is calculated as

$$\varepsilon_v = \frac{\Delta V}{V} = \varepsilon_{11} + 2\varepsilon_{33}$$

Principal strain difference is calculated as

$$P\varepsilon D = \varepsilon_{11} - \varepsilon_{33}$$

Composite plots of test data from the triaxial shear tests are shown in Figures 1, 2, and 3. Figure 1 shows the stress paths for the triaxial shear tests. This plot indicates the increase in shear capacity of the concrete as the hydrostatic stress increases. The PSD at the 200-MPa confining stress level is approximately twice that observed at the 50-MPa confining stress level. Figure 2 shows the stress-strain response of the concrete during the triaxial shear phase of the tests. These data show the ductile nature of the response of HSPC concrete under states of high confining stress. The volumetric response of the material (Figure 3) is characterized by volumetric compaction during the hydrostatic compression portion and dur-

TABLE 3 Results of Characterization Tests: PP/HSPC-1

Test Name	Test Type	Length (mm)	Diameter (mm)	Length-Diameter Ratio	Maximum Radial Stress, $\sigma_{33\ max}$ (MPa)	Maximum Axial Stress, $\sigma_{11\ max}$ (MPa)	Maximum Axial Strain, $\varepsilon_{11\ max}$, at $\sigma_{11\ max}$ (%)	PSD at $\sigma_{11\ max}$ (MPa)	MNS at $\sigma_{11\ max}$ (MPa)
CTC75-1	Triaxial Shear	88.9	53.6	1.66	50	257	1.5	207	121
CTC145-1	Triaxial Shear	88.5	51.0	1.73	100	408	10.0	308	203
CTC21-2	Triaxial Shear	88.5	53.6	1.65	150	540	10.0	390	274
CTC30-1	Triaxial Shear	88.9	53.6	1.66	200	631	10.0	431	346
UX-1	Uniaxial Strain	88.5	51.0	1.73	236	499	2.0	263	324
UX-2	Uniaxial Strain	88.9	53.6	1.66	235	493	2.4	258	321

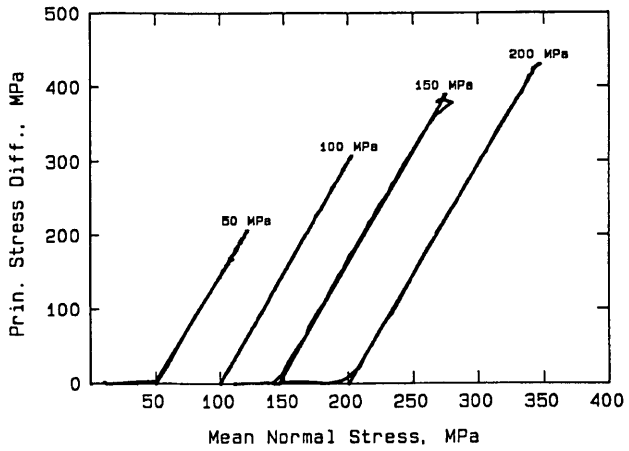

FIGURE 1 Triaxial shear test results, principal stress difference versus mean normal stress, PP/HSPC-1.

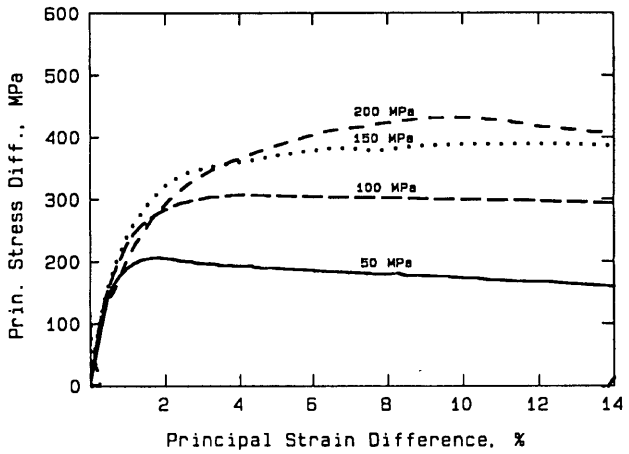

FIGURE 2 Triaxial shear test results, principal stress difference versus principal strain difference, PP/HSPC-1.

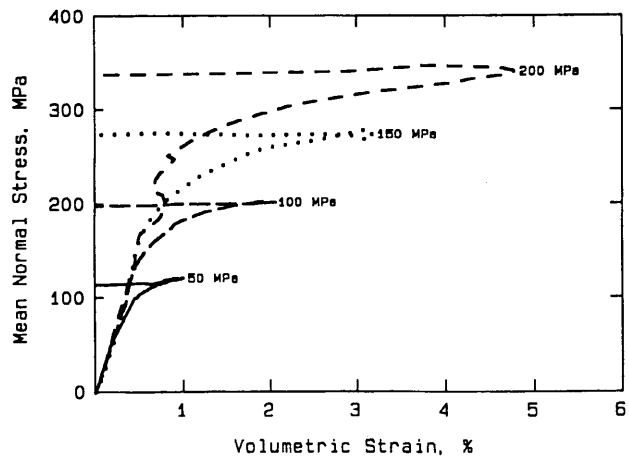

FIGURE 3 Triaxial shear test results, mean normal stress versus volumetric strain, PP/HSPC-1.

ing the initial stages of the triaxial shear loading. However, as can be seen in the Figure 3, for each confining stress level, a certain point is reached beyond which shear dilatancy initiates abruptly.

In Figures 4 and 5, composite data from the uniaxial strain tests have been plotted. From these data it can be observed that slope of the MNS versus ε_v curve is essentially bilinear, with the initial slope being stiffer than the final slope.

Analysis

Several salient features of the response of HSPC concrete to multiaxial stress states can be observed from these data. The overall multiaxial response of HSPC concrete is not significantly different from that of normal-strength concretes. HSPC concrete is typically considered to be a brittle material. However, these test data show that HSPC concrete is capable of

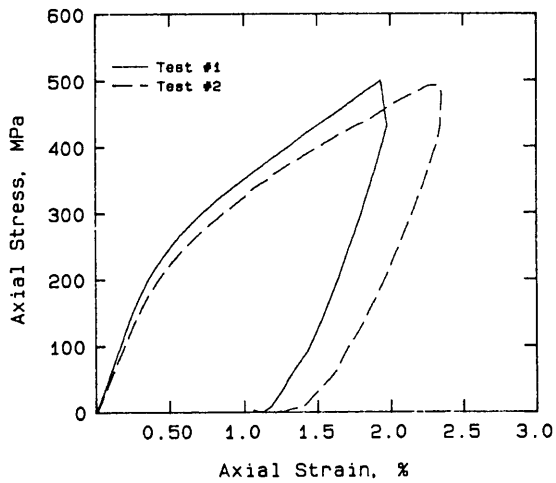

FIGURE 4 Uniaxial strain test results, axial stress versus axial strain, PP/HSPC-1.

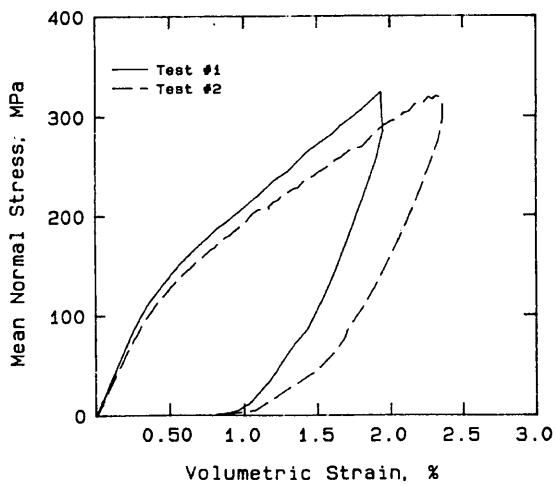

FIGURE 5 Uniaxial strain test results, mean normal stress versus volumetric strain, PP/HSPC-1.

large plastic strains and ductile flow under states of high confinement. The material exhibits strain-softening ductile behavior at the 50-MPa level. At confining stresses of 100 MPa and greater, the material behavior is characterized by a strain-hardening ductile behavior to axial strains of 10 percent or greater. The volumetric response under states of triaxial shear is characterized by shear compaction up to a point of minimum volume, followed by rapid onset of shear dilatancy. The uniaxial strain response is similar to that of normal-strength concretes.

In Figure 6 failure data obtained in the triaxial shear tests up to 200-MPa confining pressure have been used to construct an interpreted failure surface in the PSD-MNS plane. The unconfined compressive strength of the mixture is also included as a point in the plot. These data are essential to the development and verification of constitutive models for predicting the multiaxial response of HSPC concrete.

Recent advances in constitutive model development for concrete have included plasticity-based models, continuous damage models, endochronic models, and others. Factors to be considered in the choice of a constitutive model for HSPC concrete include the abilities to predict

- Strain-softening ductile behavior,
- Strain-hardening ductile behavior, and
- Shear dilatancy.

As tabulated in Table 3, the length-to-diameter ratios (L/D) for the test specimens were in the range of 1.65 to 1.73. Ideally, these ratios should be approximately 2 or greater. The effect of the low L/D ratio on the outcome of the tests cannot be quantified.

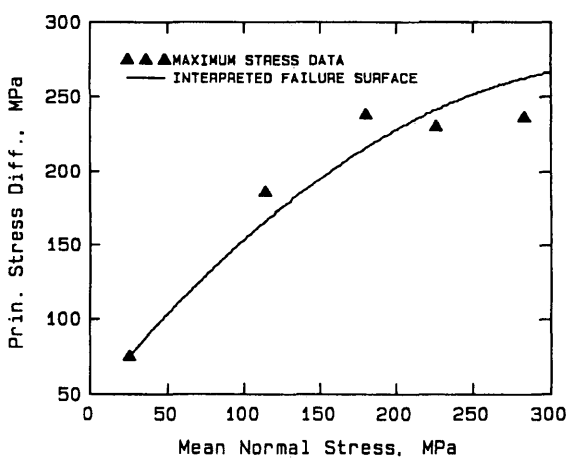

FIGURE 6 Triaxial shear test failure data and interpreted failure surface.

CONCLUSIONS

Multiaxial response characterization tests were conducted on an HSPC concrete mixture with a water-cement ratio of 0.23 and an unconfined compressive strength of 105 MPa at 56 days of age. The concrete mixture proportions were selected from readily available materials. The triaxial response tests were conducted along triaxial shear and uniaxial strain paths. Triaxial shear tests were conducted at confining stresses of 50, 100, 150, and 200 MPa. Stress-strain response data as well as failure data were obtained in the tests. The test results show that HSPC concrete, usually considered to be a brittle material, is capable of large plastic strains and ductile flow under states of high confinement. To capture the essential features of the multiaxial response of HSPC concrete, a constitutive model should be capable of predicting strain-softening ductile response, strain-hardening ductile response, and shear dilatancy.

ACKNOWLEDGMENTS

The tests described and the resulting data presented herein, unless otherwise noted, were obtained from research conducted under the Hardened Structures Research Program of the U.S. Army Corps of Engineers by the Waterways Experiment Station. Permission was granted by the Chief of Engineers to publish this information.

REFERENCES

1. K. L. Saucier. *High-Strength Concrete Past, Present, and Future.* Miscellaneous Paper SL-79-12. U.S. Army Engineer Waterways Experiment Station, Vicksburg, Miss., May 1979.
2. K. L. Saucier, W. O. Tynes, and E. F. Smith. *High Compressive Strength Concrete, Report 3, Summary Report.* Miscellaneous Paper 6-520. U.S. Army Engineer Waterways Experiment Station, Vicksburg, Miss., March 1984.
3. A. A. Bombich and A. D. Magoun. *Optimization of High-Strength Concrete Mixture Proportions for the ANMCC Improvement Project.* Miscellaneous Paper SL-82-12. U.S. Army Engineer Waterways Experiment Station, Vicksburg, Miss., Aug. 1982.
4. K. L. Saucier. *High-Strength Concrete for Peacekeeper Facilities.* Miscellaneous Paper SL-84-3. U.S. Army Engineer Waterways Experiment Station, Vicksburg, Miss., March 1984.
5. B. D. Neeley, M. I. Hammons, and D. M. Smith. *The Development and Characterization of Conventional-Strength and High-Strength Concrete Mixtures for Projectile Penetration Studies.* Technical Report SL-91-15. U.S. Army Engineer Waterways Experiment Station, Vicksburg, Miss., Aug. 1991.
6. M. I. Hammons, B. D. Neeley, and D. M. Smith. *The Development and Characterization of Fiber-Reinforced and Slag-Binder Concrete Mixtures for Projectile Penetration Studies.* Technical Report SL-92-16. U.S. Army Engineer Waterways Experiment Station, Vicksburg, Miss., June 1992.

Publication of this paper sponsored by Committee on Mechanical Properties of Concrete.